J Solid State Electrochem (1997) 1: 36–44

ORIGINAL PAPER

Keith B. Oldham

Steady-state electrolysis at a grooved or ridged plane

Received: 27 September 1996 / Accepted: 11 March 1997

Abstract This study concerns an infinite plane whose smoothness is marred by a single defect: either a groove or a ridge. The blemished plane serves as an electrode supporting a diffusion-controlled steady-state process. By using a convenient coordinate transformation, the local current density at all points on the surface is determined exactly. The results are found to confirm intuitive expectations. Thus, compared with normal values on the plane remote from a groove, the electron transfer rate is diminished within the groove but enhanced along its margins. Similarly, an abnormally large transfer rate is encountered high on the ridge but the rate is subnormal on its lower flanks. The total current is demonstrated to be unchanged by the presence of the blemish.

Key words Electrolysis · Current density · Groove · Ridge

Introduction

The rate of an electron-exchange reaction on a solid electrode depends on a variety of factors, including many that relate to the chemical and physical properties of the substrate. However, the geometry of the electrode can also exert considerable influence on the reaction rate, and it is important in any study of solid-state electrochemistry to be certain that this geometric factor is excluded before differences in local current density are attributed to intrinsic properties of the solid. This article provides an answer to the question of how a small departure from a regular geometry, a departure which may be mild enough to escape detection, will influence the rate of an electrode reaction that would otherwise be uniform spatially and invariant with time. Because interest is focused on the electrode shape, other aspects of the electrode process are as simple as possible: steady-state diffusive transport with total concentration polarization but without ohmic polarization.

The simplest electrode geometry is the infinite plane, and many electrochemical techniques were devised on the basis of this idealized system [1]. Practical electrodes may depart from the simple model because they have edges that need to be taken into account (unless the electrode is ''shielded'' or unless the linear dimension of the electrode vastly exceeds the ''distance scale'' of the experiment) and also because practical electrodes will not have the infinite smoothness of the mathematical model. It is to the second of these departures that this article is addressed. Following the classical work of deLevie [2], there continues to be great interest [3–17] in modeling electrochemistry at electrodes that are uniformly ''rough'', a popular contemporary trend being to treat fractally rough surfaces [18–26]. As with a recent investigation [27] of the effect of a notch on an otherwise flat electrode, the present study will analyze the effect of a *single* blemish, a groove or a ridge, on the surface of an otherwise mirror-smooth plane. How this imperfection affects the current density in its vicinity will be derived by an exact, analytical, approach.

The problem to be solved

Here attention is directed to an electrochemical system in which the overwhelming majority of the surface of a working electrode is an infinite flat plane, but a single linear groove or ridge, such as might arise from an unintended scratch or crease, sullies that surface. We seek to determine how this blemish affects the current density in its vicinity. Remote from the groove or ridge, both in the solution and at the electrode, the current density will be uniform, directed perpendicularly to the electrode, and will have its constant ''normal'' value i_∞.

K. B. Oldham
Chemistry Department, Trent University, Peterborough, Ontario, K9J 7B8, Canada

The flow of electricity is maintained in the steady state by the linear concentration gradient of a diffusing electroreactant with respect to which the electrode is totally concentration polarized.

A cartesian coordinate system may be erected such that $z = 0$ is the plane of the majority of the electrode, most or all of the solution phase occupying positive z values. The x axis is aligned with the direction of the blemish, so that there is translational symmetry along the x direction. The origin of the y axis is chosen such that $y = 0$ marks the location of the nonplanar feature. To learn about how the groove or ridge perturbs the otherwise simple diffusional situation, we seek to solve the steady-state two-dimensional version of Fick's second law

$$\frac{\partial^2 c}{\partial y^2} + \frac{\partial^2 c}{\partial z^2} = \nabla^2 c = \frac{1}{D}\frac{\partial c}{\partial t} = 0 \tag{1}$$

subject to the following boundary conditions:

$$c = 0 \text{ at the electrode surface} \tag{2}$$

$$\frac{\partial c}{\partial z} = \text{constant} = \frac{i_\infty}{nFD} \text{ as } z \to \infty \tag{3}$$

$$\frac{\partial c}{\partial z} = \text{constant} = \frac{i_\infty}{nFD} \text{ as } y \to \pm\infty \tag{4}$$

and

$$\frac{\partial c}{\partial y} = 0 \text{ as } y \to \pm\infty \tag{5}$$

The terms n, F and D have their usual significances: n is the number of electrons involved in the electrode reaction, F is Faraday's constant and D is the diffusivity (diffusion coefficient) of the electroreactant. Boundary conditions Eqs.3 and 4 arise from recognizing that, close to the electrode but far from the imperfection, the steady-state concentration profile will be linear

$$c = \text{ (constant) } z = \frac{\partial c}{\partial z} z = \frac{i_\infty z}{nFD} \tag{6}$$

Obviously, the linearity of the concentration profile cannot, in practice, extend to infinity as Eq. 3 supposes. The final equality in Eq. 6 is imposed to satisfy the requirements of Fick's first law and Faraday's law.

Of course, in the absence of a defect, Eq. 6 holds at *all* locations on the plane. The strategy to be adopted for finding concentrations close to the blemished plane will be to transform the boundary value problem so that an equation analogous to Eq. 6 holds globally.

Geometry of the blemish

There is a myriad of possible geometries that the groove or ridge might adopt. Here the chosen shape of the blemish in the y, z plane is that described by

$$y^2 = \left[1 + \frac{\sqrt{w^2 + h^2}}{2z}\right][h - z]\left[z - h + \frac{\sqrt{w^2 + h^2}}{2}\right] \tag{7}$$

where w is a positive length parameter and h is a nonzero length of either sign. This is certainly not the simplest geometry for a groove or ridge; our choice is made for mathematical felicity, as will be evident later. Figure 1 shows, to scale, the profiles of several grooves and ridges that conform to this equation. The number associated with each profile is its "shape factor" β, defined by

$$\beta = \frac{8h\sqrt{w^2 + h^2}}{\left[\sqrt{w^2 + h^2} - 2h\right]^2} \tag{8}$$

which takes values in the range $-1 \le \beta \le \infty$. The diagram shows no examples for shape factors within the range $-0.5 < \beta < 5$, not because these are uninteresting

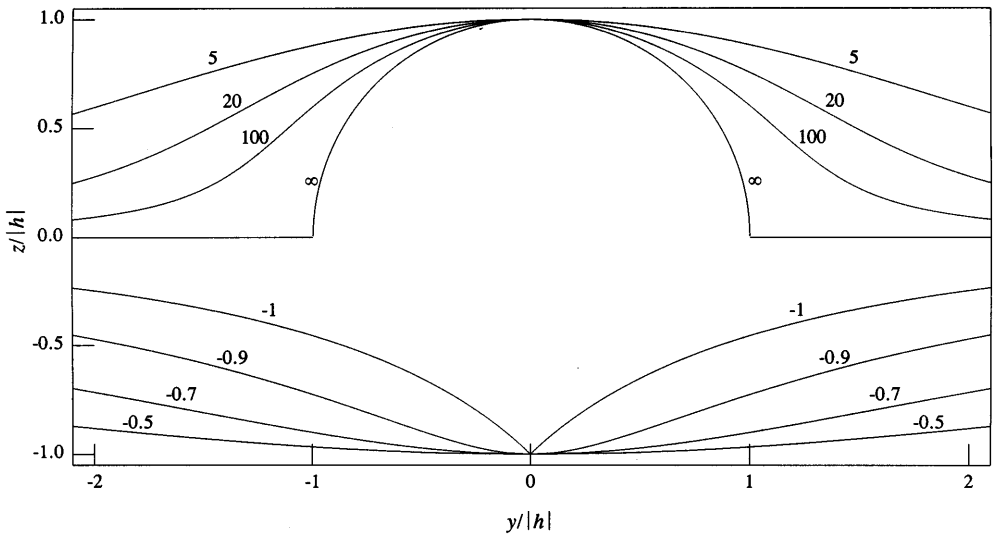

Fig. 1 Shapes of grooves and ridges for the shape factors β as indicated. Both ordinate and abscissa have been normalized by division by $|h|$, the Lees feature's depth or height, so that the profiles are depicted "to scale"

– on the contrary, values in this range are the most likely to occur with inadvertently flawed "flat" electrodes – but because such profiles are too shallow for effective pictorial portrayal.

In Eq. 7 and elsewhere, $\sqrt{w^2+h^2}$ is understood to represent a positive length, even if h is negative. This equation describes a feature with bilateral symmetry about the plane $y=0$. The profile is simple only if $w \geq \sqrt{3}|h|$, which inequality is therefore imposed. When h is positive, Eq. 7 represents a ridge, with h being the height of the ridge and w its width at half-height. Negative values of h correspond to a groove of depth $-h$, with w being the width at half-depth. Thus Eq. 7 is satisfied by $(y=0, z=h)$ and by $(y=\pm 1/2w, z=1/2h)$. We shall describe such a profile as a "Lees feature" to acknowledge the work of a pioneer who used equations of this form to study terrestrial temperature distributions in mountainous regions [28].

The equation of a Lees feature simplifies to

$$y^2 = \frac{\beta a^2 (a+z)}{4z} - (a+z)^2 \tag{9}$$

in terms of the dimensionless shape factor β and a characteristic positive length defined by

$$a = \frac{\sqrt{w^2+h^2}}{2} - h \tag{10}$$

The inequality $w \geq \sqrt{3}|h|$ becomes replaced by $-1 \leq \beta \leq \infty$. Grooves correspond to $-1 \leq \beta < 0$, whereas ridges are characterized by $0 < \beta \leq \infty$. Note that as $\beta \to \infty$, the product βa^2 remains finite and becomes equal to $4h^2$. In terms of the β and a parameters, the dimensions of the Lees feature are

$$h = \frac{a\left(\sqrt{1+\beta}-1\right)}{2} \tag{11}$$

and

$$w = \frac{a\sqrt{6+10\sqrt{1+\beta}+3\beta}}{2} \tag{12}$$

Note that, at constant β, altering a causes both the height and width of the blemish to change proportionately, so that its shape remains unchanged.

The dimensions of the blemishes portrayed in Fig. 1 have been normalized in this diagram by division by $|h|$, their maximum height or depth. It is evident that the profiles are generally smooth curves, but that this is not the case at each end of the permitted range of shape factors. When $\beta=-1$ there is a sharp discontinuity with a dihedral angle of 90°, so that the term "notch" might be a better descriptor of this shape than "groove". The equation of the profile in this limiting case is

$$y^2 = \frac{(a+z)(a+2z)}{-4z} = (h-z)^2\left[\frac{2h}{z}-1\right] \tag{13}$$

Similarly, Fig. 1 shows the limiting case for a ridge-like blemish. This corresponds to $\beta \to \infty$ as $a \to 0$, but is more easily recognized in the unsimplified Eq. 7 on setting $w=\sqrt{3}h$. The limiting ridge has two 90° edges, obeys the simple equation

$$y^2 = h^2 - z^2 \text{ when } |y| < h \tag{14}$$

and is, in fact, a hemicylinder resting on the infinite plane.

The gradient $\tan\{\theta\}$ of the surface at any point (y,z) on the electrode equals $\mathrm{d}z/\mathrm{d}y$. Its reciprocal may be found via straightforward differentiation of Eq. 9:

$$\frac{\mathrm{d}y}{\mathrm{d}z} = \frac{-\beta a^3}{8z^2 y} - \frac{a+z}{y} = \cot\{\theta\} \tag{15}$$

Squaring this result and adding unity now gives

$$\csc^2\{\theta\} = \frac{\beta^2 a^6 + 16\beta a^2 (a+z)^2 z^2}{64 z^4 y^2} \tag{16}$$

after some algebra. One interpretation of this result is that, if n represents distance measured along the normal into the solution phase from a point (y,z) on the electrode, then

$$\frac{\mathrm{d}n}{\mathrm{d}y} = -\csc\{\theta\} = \pm\frac{a\sqrt{\beta^2 a^4 + 16\beta(a+z)^2 z^2}}{8z^2 y} \tag{17}$$

where the upper/lower signs relate to the ridge/groove alternatives. Note that these signs were selected because $(\mathrm{d}n/\mathrm{d}y)$ for the groove is clearly negative when y is positive, whereas $(\mathrm{d}n/\mathrm{d}y)$ is positive for the ridge geometry. The diagrams in Fig. 2 will clarify these arguments. The equations of this paragraph will find use later.

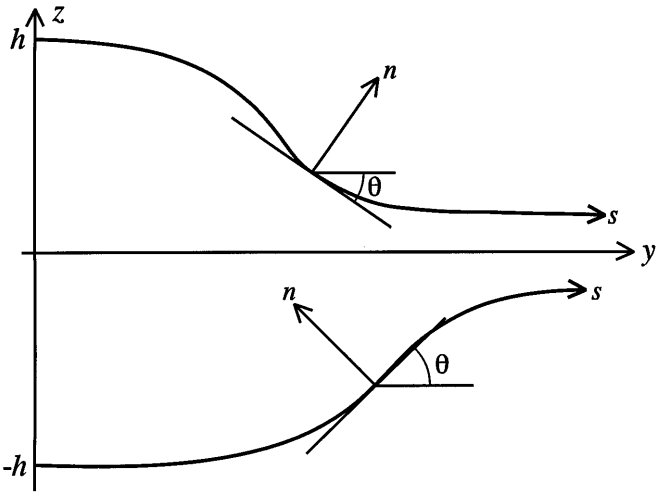

Fig. 2 Diagrams showing the relationships between the angle θ and the normal dimension n for a ridge (*upper diagram*) and a groove. The angle θ is negative for the ridge. s is a length measured along the feature's surface from its intersection with the z-axis

Solution for concentration

Following Lees, let us now define a set of modified coordinates Y, Z. These are related to the cartesian y, z coordinates by

$$Y = y + \frac{\beta a^2 y}{4\left[y^2 + (a+z)^2\right]} \tag{18}$$

and

$$Z = z - \frac{\beta a^2 (a+z)}{4\left[y^2 + (a+z)^2\right]} \tag{19}$$

The changes in the coordinate system may be considered to arise from the introduction of a source/sink doublet [29] positioned at the point $y = 0, z = -a$. These new coordinates have three properties which make them valuable for our purpose. First, $Z = 0$ corresponds to Eq. 9, and therefore describes the electrode surface. Our interest is confined to $Z \geq 0$ and $-\infty < Y < \infty$. Second, Y and Z become identical with the cartesian coordinates y and z respectively, as $z \to \infty$, and/or $y \to \pm\infty$, i.e. far from the Lees feature, where the concentration distribution is described by the simple boundary conditions (Eqs. 3–5). And third, it is straightforward to demonstrate that Y and Z satisfy the Cauchy-Riemann equations [30]

$$\frac{\partial Z}{\partial z} = \frac{\partial Y}{\partial y} \text{ and } \frac{\partial Z}{\partial y} = -\frac{\partial Y}{\partial z} \tag{20 and 21}$$

establishing that Y and Z are mutually orthogonal. Figure 3 compares the two coordinate systems for the case $\beta = 100$.

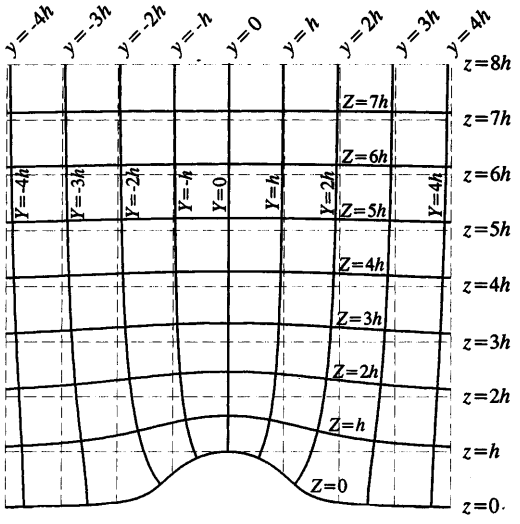

Fig. 3 The coordinate system for the $\beta = 100$ ridge. *Full lines* represent the modified coordinates Y, Z and *broken straight lines* are the cartesian y, z coordinates with which they merge at large distances from the origin

The Y, Z coordinates constitute the ideal framework on which to solve our problem. The differential Equation 1 and its attendant boundary conditions (Eqs. 2–5) translate directly to

$$\frac{\partial^2 c}{\partial Y^2} + \frac{\partial^2 c}{\partial Z^2} = \nabla^2 c = \frac{1}{D}\frac{\partial c}{\partial t} = 0 \tag{22}$$

$$c = 0 \text{ at } Z = 0 \tag{23}$$

$$\frac{\partial c}{\partial Z} = \text{constant} = \frac{i_\infty}{nFD} \text{ as } Z \to \infty \tag{24}$$

$$\frac{\partial c}{\partial Z} = \text{constant} = \frac{i_\infty}{nFD} \text{ as } Y \to \pm\infty \tag{25}$$

and

$$\frac{\partial c}{\partial Y} = 0 \text{ as } Y \to \pm\infty \tag{26}$$

Now compare these five equations with the Eq. set 1–5. The Lees problem in Y, Z coordinates is seen to correspond exactly to the unblemished plane in y, z coordinates. Thus, by analogy with Eq. 6, it is possible immediately to recognize

$$c = \frac{i_\infty Z}{nFD} \tag{27}$$

as the simple solution to the Eq. set 22–26. Figure 4 illustrates the equiconcentration surfaces for the $\beta = -0.64$ case.

Solution for current density

The magnitude i of the local current density at the electrode surface may now be found from the gradient $\partial c/\partial Z$ via the formula

$$i = \frac{nFD}{h_{Z=0}}\left(\frac{\partial c}{\partial Z}\right)_{Z=0} \tag{28}$$

which incorporates both Faraday's law and Fick's first law. Here $h_{Z=0}$ is the metric, or scale factor [31], of the Z coordinate at the electrode surface. Combination of the last two equations shows that

$$\frac{i}{i_\infty} = \frac{1}{h_{Z=0}} \tag{29}$$

The metric is defined in terms of the distance covered as one moves away normally from the electrode surface into the solution; if fact $h_{Z=0}$ is simply $(\partial n/\partial Z)_Y$ where n is the vector length from a point (y, z) on the surface measured along the normal into the solution phase, as introduced earlier. It follows that

$$\frac{i}{i_\infty} = \left(\frac{\partial Z}{\partial n}\right)_Y = \frac{\left(\frac{\partial Z}{\partial y}\right)_Y}{\left(\frac{\partial n}{\partial y}\right)_Y} \tag{30}$$

The $\partial n/\partial y$ term in this formula is available from Eq. 17, but it is not trivial to evaluate $(\partial Z/\partial y)_Y$.

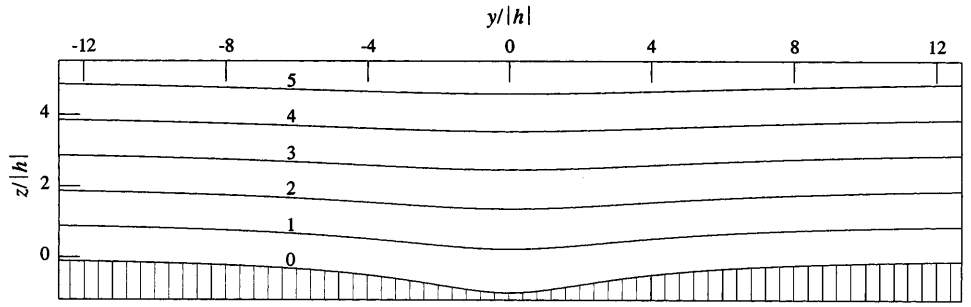

Fig. 4 Equiconcentration surfaces close to a grooved $\beta = -0.64$ electrode. The *numbers associated with each curve* represent $nFDc/i_\infty|h|$, where c is the local concentration

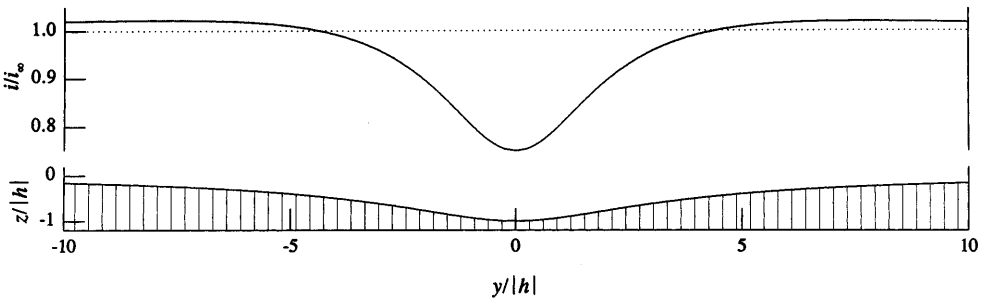

Fig. 5 The *lower curve* shows the profile of a grooved electrode for which the shape factor β equals -0.64. The *upper curve* shows the corresponding ratio of i, the local current density, to i_∞, which is the current density at a point on the plane remote from the groove

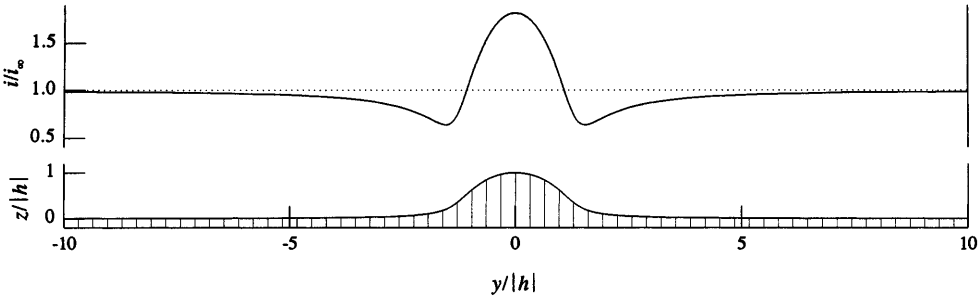

Fig. 6 As Fig. 5, but for the $\beta = 100$ ridge. In both figures, and in Figs. 8 and 9, the *lower curves* represent the true profiles of the grooves, i.e. the scales of the y- and z-coordinates are the same

We start with the equation

$$(Z+a)^2 = (2y-Y)^2\left[\frac{\beta a^2}{4y(Y-y)} - 1\right] \tag{31}$$

which can be derived by eliminating all z terms between the definitions 18 and 19. Then, differentiation with respect to y gives

$$2(Z+a)\left(\frac{\partial Z}{\partial y}\right)_Y = \frac{\beta a^2 Y^2(2y-Y)}{4y^2(Y-y)^2} - 4(2y-Y) \tag{32}$$

Next we replace each Y term by $2y-(a+Z)y/(a+z)$, this equivalence being a consequence of the definitions of the modified coordinates. Finally, on setting $Z=0$, the result

$$\left(\frac{\partial Z}{\partial y}\right)_{Y,Z=0} = \frac{\beta a^2(a+2z)^2}{8(a+z)z^2y} - \frac{2y}{a+z} \tag{33}$$

emerges. This expression applies along the normal, at any point (y,z) on the electrode. Accordingly, it may be reformulated as

$$\left(\frac{\partial Z}{\partial y}\right)_{Z=0} = \frac{\beta a^4 + 16(a+z)^2z^2}{8(a+z)z^2y} \tag{34}$$

by exploiting relationship 9.

A final expression for the normalized local current density arises by substituting from Eqs. 34 and 17 into Eq. 30. After rearrangements, one finds

$$\frac{i}{i_\infty} = \sqrt{\frac{a^2}{(a+z)^2} + \frac{16z^2}{\beta a^2}} \tag{35}$$

or, in terms of the dimensions of the feature

$$\frac{i}{i_\infty} = \sqrt{\frac{\left[\frac{\sqrt{w^2+h^2}}{2} - h\right]^2}{\left[\frac{\sqrt{w^2+h^2}}{2} - h + z\right]^2} + \frac{8z^2}{h\sqrt{w^2+h^2}}} \tag{36}$$

We have chosen to express the current density i at a point on the electrode as a function of the z-coordinate of that point. In principle, a rather more useful formulation would be in terms of the y-coordinate, but we

have avoided this to circumvent the solution of awkward cubic equations.

Equation 35 is a remarkably simple result. Figures 5 and 6 show the distribution of current densities for typical Lees features, one example each of a groove and a ridge. Note that there is qualitative agreement between these diagrams and intuitive expectations: the current density is generally larger than normal where the surface is convex, but less than normal where it is concave. There is not a one-to-one correlation between current density and curvature, however; thus the two isolated points at which $i = i_\infty$ are *not* the inflection points of the profiles. Some quantitative implications of Eq. 35 will now be addressed. Its special cases will receive attention later.

Extreme current densities

As would be expected, the minimum current density at a groove occurs at the bottom of the groove, and the current density at a ridge is maximal at its peak. Hence the extremum i_{ext} in the current density is always found at $(y = 0, z = h)$. Substitution of $z = h$ into Eq. 35 leads to the formula

$$\frac{i_{\text{ext}}}{i_\infty} = \sqrt{\frac{a^2}{(a+h)^2} + \frac{16h^2}{\beta a^2}} = \frac{2}{1 + \frac{1}{\sqrt{1+\beta}}} = 1 + \frac{2h}{\sqrt{w^2 + h^2}} \tag{37}$$

which exhibits a very simple dependence on the shape factor. Some values of the extreme current density are listed in Table 1, as a function of β and of the corresponding height/width ratio. The behavior is seen to be pleasingly simple in that the current density ranges from 100% less than normal to 100% more than normal as one proceeds through Lees features from the most pronounced groove to the most pronounced ridge. Moreover, the extreme currents at a ridge and a groove having the same $|h|/w$ ratio invariably average to i_∞.

Table 1 The current density displays a minimum or a maximum at $y = 0$. Values of this extreme value i_{ext}, compared to the current density i_∞ remote from the defect, are shown here for various values of the ratio of the height (or depth) of the blemish to its width.

h/w	β	i_{ext}/i_∞
−0.5774	−1	0
−0.5	−0.997	0.106
−0.4	−0.978	0.257
−0.3	−0.927	0.425
−0.2	−0.809	0.608
−0.1	−0.554	0.801
0	0	1
0.1	1.271	1.199
0.2	3.984	1.392
0.3	12.709	1.575
0.4	44.907	1.743
0.5	320.997	1.894
0.5774	∞	2

If we continue to refer to i_∞ as the "normal" current density, then Table 1 confirms that the current density at $y = 0$ is subnormal for a groove and supernormal for a ridge. However, as one proceeds away from $y = 0$, one eventually encounters the opposite behavior: a supernormal current density for a groove and a subnormal current density for a ridge. That this is so is evident on making a power series expansion of Eq. 35. The first few terms are

$$\frac{i}{i_\infty} = 1 - \frac{z}{a} + \frac{(8\beta + 1)z^2}{a^2} + \frac{(8\beta - 1)z^3}{a^3} + \dots \tag{38}$$

Because z is invariably negative for a groove, one sees that when the magnitude of z is sufficiently small, then $i > i_\infty$. Conversely, because z is positive for a ridge, i will be subnormal at a sufficiently large distance from the origin.

Total current

The total current may be found by integrating the current density over the surface of the blemished plane. Let I be the current arising from a strip of width L in the x-direction, then

$$I = \int_0^L \int_{-\infty}^{\infty} i \, \mathrm{d}s \, \mathrm{d}x = L \int_{-\infty}^{\infty} i \, \mathrm{d}s \tag{39}$$

Here s denotes distance measured from the symmetry plane along the electrode surface, as Fig. 2 illustrates. Because I is, of course, infinite, it is the difference between the current at the grooved or ridged electrode and that, I_{plane}, at an unblemished planar electrode that is accessible. In fact, it is the quantity

$$\frac{I - I_{\text{plane}}}{Lwi_\infty} = \frac{1}{wi_\infty}\left[\int_{-\infty}^{\infty} i \, \mathrm{d}s - \int_{-\infty}^{\infty} i_\infty \mathrm{d}y\right] \tag{40}$$

that will be evaluated. This is a suitably normalized quantity reflecting the difference in total current caused by the groove or ridge.

In the limiting steady state, the total current is controlled by factors dissociated from the electrode surface, and one may therefore expect that the presence of the Lees feature will not have affected the total current. Thus an astute prediction is that the quantity in Eq. 40 will be zero. Establishing that this is, indeed, true will validate our treatment.

By analogy with the discussion surrounding Eq. 15, aided by inspection of Fig. 2, it follows that

$$\begin{aligned} \mathrm{d}s &= \left[\sqrt{(\mathrm{d}y)^2 + (\mathrm{d}z)^2}\right]_{Z=0} \\ &= \left[\sqrt{1 + \left(\frac{\mathrm{d}z}{\mathrm{d}y}\right)^2}\right]_{Z=0} \mathrm{d}y = \sec\{\theta\}\ \mathrm{d}y \end{aligned} \tag{41}$$

On combining the last two equations, and recognizing the symmetry about the $y = 0$ plane, we arrive at

$$\frac{I - I_{\mathrm{plane}}}{Lwi_\infty} = \frac{2}{wi_\infty}\int_0^\infty (i\sec\{\theta\} - i_\infty)\ \mathrm{d}y \tag{42}$$

or equivalently, since $\mathrm{d}y = \cot\{\theta\}\ \mathrm{d}z$

$$\frac{I_{\mathrm{plane}} - I}{Lwi_\infty} = \frac{2}{w}\int_h^0 \left[\frac{i}{i_\infty}\csc\{\theta\} - \cot\{\theta\}\right]\mathrm{d}z \tag{43}$$

Expressions for $i/i_\infty, \csc\{\theta\}$ and $\cot\{\theta\}$ are available from Eqs. 35, 17 and 15. When these are inserted into Eq. 43, and y is then replaced by recourse to Eq. 9, one finds that

$$\frac{I_{\mathrm{plane}} - I}{Lwi_\infty} = \frac{1}{2w}\int_0^h \frac{8(a+z)^2 z - \beta a^3}{\sqrt{\beta a^2(a+z)^3 z - 4(a+z)^4 z^2}}\mathrm{d}z \tag{44}$$

is the expression that is expected to evaluate to zero. Unfortunately, this complicated integral has defied analytical solution. However, taking $\beta = -0.64$, which corresponds to a typical groove, the equivalent summation

$$\frac{2}{\sqrt{63}}\sum_\zeta \frac{[10 + (5+\zeta)^2\zeta]\Delta}{\sqrt{-\zeta(5+\zeta)^3(4+5\zeta+\zeta^2)}} \tag{45}$$

in which ζ replaces z/h and takes the values $\Delta, 2\Delta, 3\Delta, \ldots, 1-\Delta$, and 1, was evaluated numerically.

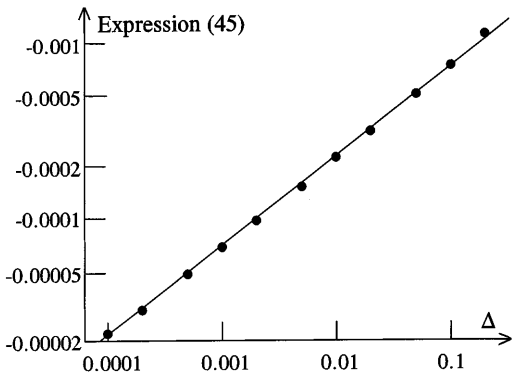

Fig. 7 The *points* in this logarithmic plot show how the magnitude of the quantity in expression 45 depends on Δ. The *line* has a slope of 0.522

Figure 7 shows how the magnitude of the quantity in expression 45 changes as Δ, the summation or integration interval, adopts progressively smaller values. Evidently the sum approaches zero steadily (interestingly, as $\sqrt{\Delta}$) as the numerical integration improves in precision. We regard this as proof that the integral in Eq. 44 vanishes and, by extension, as a vindication of the treatment.

Limiting cases

Though their existence is incidental to the main purpose of this article, the two values of the shape factor β that mark the limits of its permitted range correspond to geometries which are sufficiently different from typical grooves and ridges to warrant special consideration. These two instances of the Lees feature, that will henceforth be refered to as the "notch" and "hemicylinder" cases, correspond to profiles with a width-to-depth or width-to-height ratio of $\sqrt{3}$. The simplified equations that describe their profiles were reported as Eqs. 13 and 14.

The current density flowing to the notch is illustrated in Fig 8 and given by

$$\frac{i}{i_\infty} = \frac{(z-h)\sqrt{h^2 + 2hz - z^2}}{h\left(\frac{z}{2} - h\right)} \tag{46}$$

which is the $\beta = -1, a = -2h$ version of Eq. 35. In interpreting Eq. 46, recognize that both h and z are negative. The current density is zero at the seat of the notch, which is consistent with the known voltammetric behaviour of right-angled grooves [32, 33]. Moving away from the notch, i rises steadily but diminishingly to become normal at $y = \pm 1.51427h,\ z = 0.328538h$. Beyond this, the current density is supernormal, reaching a maximum value of $1.038786i_\infty$ at $y = \pm 2.83929h,\ z = 0.160713h$ before declining back towards normality.

Turning to the other limit, the hemicylindrical case, we find that the expression for the current density is even simpler. When the parameter limits $a \to 0$, $\beta a^2 \to 4h^2$ are taken, Eq. 35 simplifies to

$$\frac{i}{i_\infty} = \frac{2z}{h} = 2\frac{\sqrt{h^2 - y^2}}{h} \quad |y| \le h \tag{47}$$

This formula is restricted to the curved portion of the surface. To evaluate the current density over the flat region of the electrode, outside the realm of the hemicylindrical blemish, first recognize that the taking of the $a \to 0, \beta a^2 \to 4h^2$ limit of Eq. 9 requires that $z \to 0$ such that

$$\frac{a}{z} = \frac{y^2 - h^2}{h^2} \quad |y| \ge h \tag{48}$$

The corresponding limit of Eq. 35 is therefore seen to be

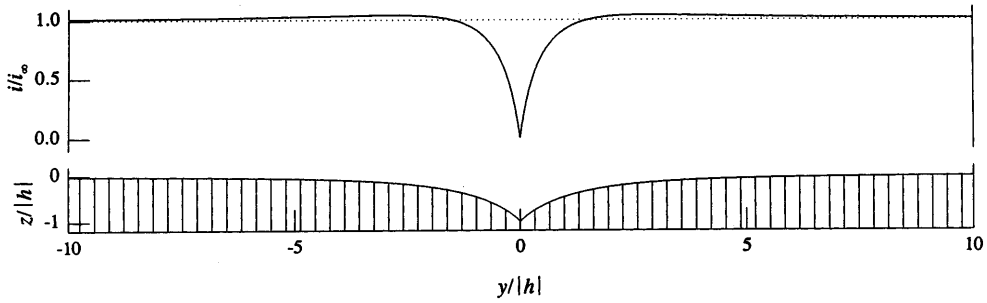

Fig. 8 As for Fig. 5, but for the "notch" case, in which $\beta = -1$

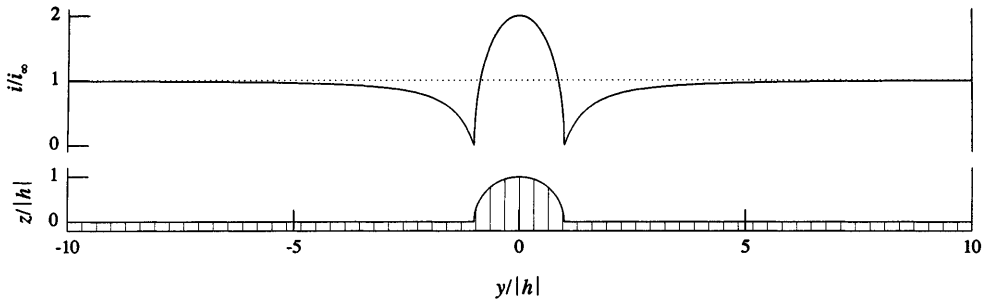

Fig. 9 As for Fig. 5, but for the hemicylinder case, in which $\beta = \infty$

$$\frac{i}{i_\infty} = \frac{y^2 - h^2}{y^2} \quad |y| \geq h \tag{49}$$

Figure 9, based on Eqs. 47 and 49, shows the current density distribution corresponding to $\beta = \infty$. The maximum current density is $2i_\infty$ on the summit of the ridge; the minimum is zero at each piedmont.

In the $\beta = \infty$ limiting case, the total current is easily found analytically. The excess current flowing to a strip of the hemicylinder of width L in the x-dimension, over and above that would flow to that region in the absence of the blemish, is

$$2L \int_0^{\pi h/2} i \, \mathrm{d}s - 2Lhi_\infty = 2Lh \left[\int_0^h \frac{i \, \mathrm{d}y}{\sqrt{h^2 - y^2}} - i_\infty \right] = 2Lhi_\infty \tag{50}$$

where the integration was accomplished with the aid of Eq. 47. This excess represents an exact doubling of the total current flowing to the blemished region $-h < y < h$. On the flat region outside the hemicylinder, the corresponding excess current is

$$2L \left[\int_{\pi h/2}^{\infty} i \, \mathrm{d}s - \int_h^{\infty} i_\infty \, \mathrm{d}y \right] = 2L \int_h^{\infty} (i - i_\infty) \, \mathrm{d}y = -2Lhi_\infty \tag{51}$$

where, in this zone, Eq. 49 provided the integrand. As expected, the excess current flowing to the hemicylinder is exactly compensated by the shortfall on the flat region adjoining the blemish.

Summary

The steady-state distribution of current density on a grooved or ridged infinite plane has been derived exactly, for shapes drawn from a class that we have termed "Lees features". Equation 36, which describes that distribution in terms of the height h and width w of a ridge, is valid for any height and any width less than $\sqrt{3}h$. The same equation holds for grooves of depth $-h$ and of any width w not exceeding $\sqrt{3}|h|$. The conclusions, of which samples are shown in Figs. 5, 6, 8 and 9, accord with, and provide quantitative support for, intuitive expectations. Compared with that on regions of the plane remote from the Lees feature, current densities are diminished in the interior of grooves and on the lower flanks of ridges, but are enhanced along the margins of the grooves and near the summits of the ridges. At the bottom of the groove, the current density may be very small, even being zero in extreme conditions. Hence, as is well known by electroplaters and electromachinists, diffusion-controlled steady-state electrodeposition may worsen surface blemishes, while electrodissolution will tend to heal such defects.

References

1. Delahay P (1954) New instrumental methods in electrochemistry. Interscience, New York
2. Levie R de (1965) Electrochim Acta 10:113
3. Halsey TC, Leibig M (1991) Electrochim Acta 36:1699
4. Louch DS, Pritzker MD (1991) J Electroanal Chem 319:33
5. Halsey TC, Leibig M (1992) Ann Phys 219:109
6. Real SG, Vilche JR, Arvia AJ (1992) J Electroanal Chem 341:181

7. Schueller GRT, Taylor SR (1992) J Electrochem Soc 139:3120
8. Louch DS, Pritzker MD (1993) J Electroanal Chem 346:211
9. Leibig M, Halsey TC (1993) J Electroanal Chem 358:77
10. Arvia AJ, lvarezza RC (1994) Electrochim Acta 39:1481
11. Jacquelin J (1994) Electrochim Acta 39:2673
12. Pajkassy T (1994) J Electroanal Chem 364:111
13. Garcia MP, Gomez MM, Salvarezza RC, Arvia, AJ (1994) J Electrochem Soc 141:2291
14. Kant R, Rangarajan SK (1994) J Electroanal Chem 368:1
15. Compton RG, Eklund JC, Page SD, Sanders GHW, Booth J (1994) J Phys Chem 98:12410
16. Gunning J (1995) J Electroanal Chem 392:1
17. Kant R, Rangarajan SK (1995) J Electroanal Chem 396:285
18. Bates JB, Chu YT (1992) Ann Biomed Eng 20:349
19. Mulder W (1992) J Electroanal Chem 326:231
20. Wang YB, Yuan RK, Yuan H, Chen ZH (1993) Synthetic Metals 55:1501
21. Zalis S, Pospisil L, Fanelli N (1993) J Electroanal Chem 349:443
22. Bidoia ED, Bulhoes LOS, Rochafilho RC (1994) Electrochim Acta 39:763
23. Chassaing E, Sapoval B (1994) J Electrochem Soc 141:2711
24. Pajkossy T, Borosy AP, Imre A, Martemyanov SA, Magy G, Schiller R, Nyikos L (1994) J Electroanal Chem 366:69
25. Larsen AE, Grier DG, Halsey TC (1995) Phys Rev E 52:R2161
26. Stromme M, Niklasson GA, Granqvist CB (1995) Phys Rev B, 52:14192.
27. O'Brien RN, Sackville PM (1993) J Electrochem Soc 140:122
28. Lees CH (1910) Proc Roy Soc A 83:399
29. Carslaw HS, Jaeger JC (1959) Conduction of heat in solids, Clarenden Press, Oxford, p 270
30. Boas ML (1983) Mathematical methods in the physical sciences. Wiley, New York, p 582
31. Speigel MR (1968) Mathematical handbook. McGraw-Hill, New York, p 124
32. Myland JC, Oldham KB (1996) J Electroanal Chem 405:39
33. Oldham KB (1996) J Electroanal Chem (in press)